Letter

Reciprocal Floquet thermalization in a one-dimensional Rydberg atom array

Yunhui He [1,2] Yuechun Jiao [1,2,*] Jianming Zhao [1,2] and Weibin Li [3,†]

[1]*State Key Laboratory of Quantum Optics Technologies and Devices, Institute of Laser Spectroscopy, Shanxi University, Taiyuan 030006, China*

[2]*Collaborative Innovation Center of Extreme Optics, Shanxi University, Taiyuan 030006, China*

[3]*School of Physics and Astronomy, and Centre for the Mathematics and Theoretical Physics of Quantum Non-equilibrium Systems, University of Nottingham, Nottingham NG7 2RD, United Kingdom*

(Received 3 June 2025; revised 10 January 2026; accepted 25 February 2026; published 16 March 2026)

Periodically driven Floquet quantum systems hold great promise for engineering exotic quantum phases and matter, but are often limited by rapid thermalization. In this work, we propose and demonstrate a square-wave-modulated Floquet engineering protocol to steer and study the thermalization dynamics in one-dimensional Rydberg atom arrays. We identify a reciprocal Floquet thermalization mechanism, which is triggered when the combination of laser detuning and Rydberg atom interactions inversely matches the Floquet period. The level statistics show narrow peaks when the reciprocal condition is met, while thermalization is suppressed between two adjacent peaks. We extract signatures of thermalization and its suppression from the stroboscopic evolution of the atomic population. Critically, thermalization occurs in a disorder-free regime, with rapid equilibration achieved within the Rydberg lifetime and experimentally accessible initial states. Our study establishes a robust framework for exploring thermalization-to-localization transitions and designing effective Hamiltonians, and highlights the unique potential of the Rydberg atom array setting for quantum simulations.

DOI: 10.1103/3gpm-9psv

Introduction. Floquet engineering [1–11] enables the realization of effective Hamiltonians and many-body phases that are often inaccessible in static Hamiltonians [12–14]. This gives an essential tool for creating quantum matter [15–19] and exploring many-body dynamics [20–22] and phases [23–28]. However, in isolated quantum systems, energy absorption from the Floquet driving often leads to heating and rapid thermalization to an effective infinite temperature thermal state [29–37], which has been observed experimentally [38–41]. Thermalization washes out correlations and suppresses nontrivial dynamics, limiting the utility of Floquet engineering [42–45]. Controlling and preventing heating, through techniques such as many-body localization [6,21,23,46–53], dynamical localization [54–56], and high-frequency driving [1,13,14,57], is important for the study of Floquet-driven quantum many-body systems.

Remarkable developments in neutral atom tweezer arrays have enabled the manipulation of long-range Rydberg interactions via sinusoidal laser detuning [58–60]. This Floquet engineering not only facilitates the study of exotic thermalization within restricted Hilbert spaces [61] but also provides a framework that is important for quantum simulation [8,62–66] and quantum computation [67–73] with the Rydberg atom array setting [74]. Despite growing interest and potentials [75–82], protocols to directly manipulate and probe Floquet thermalization in the Rydberg atom arrays remain largely unexplored.

In this work, we propose an experimentally accessible Floquet engineering scheme to efficiently manipulate and control thermalization and localization in a Rydberg atom array. The protocol employs square-wave-modulated laser fields, which periodically couple the electronic ground and Rydberg states with alternating high-(Ω_0) and low-($\Omega_l \ll \Omega_0$) Rabi frequencies of duration $\tau = T/2$ (T is the period) [Fig. 1(a)]. Varying the laser detuning Δ induces a sequential onset of many-body quantum chaos (MBQC) in the system. The chaotic regime is realized when the nearest-neighbor (NN) van der Waals (vdW) interaction V_0 is commensurate with Ω_0. Under an optimal condition $\Delta_0 T = 2K\pi$ ($\Delta_0 = \Delta + V_0$ and K is an integer), the Floquet eigenphases follow the circular orthogonal ensemble (COE) [29], reflecting the MBQC. Dynamically, this leads to a *reciprocal Floquet thermalization*, triggered by energy absorption [Fig. 1(b)], where the atomic population saturates to near zero [Fig. 1(c)]. Crucially, the effect arises in a disorder-free array, uses experimentally accessible time-dependent laser fields and initial states, and develops on timescales within the Rydberg lifetime. By combining Floquet engineering with precise control over Rydberg atom interactions, our study establishes a route for observing and steering Floquet thermalization and engineering effective many-body dynamics in Rydberg atom arrays [81].

Floquet-driven Rydberg atom array setting. Our system is a one-dimensional array of N atoms with open boundary

*Contact author: ycjiao@sxu.edu.cn

†Contact author: weibin.li@nottingham.ac.uk

Published by the American Physical Society under the terms of the Creative Commons Attribution 4.0 International license. Further distribution of this work must maintain attribution to the author(s) and the published article's title, journal citation, and DOI.

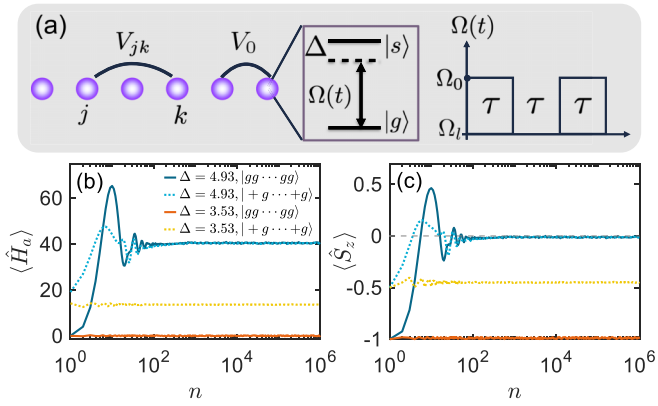


FIG. 1. (a) Floquet-driven Rydberg atom array. Atoms are coupled from the ground state $|g\rangle$ to Rydberg state $|s\rangle$ by a laser with detuning Δ and time-dependent Rabi frequency $\Omega(t)$. The latter forms a pulse train between Ω_l and Ω_0 with a period $T = 2\tau$. Rydberg atoms interact through the vdW interaction V_{jk}. By controlling detuning Δ and NN interaction V_0, the Floquet dynamics can be altered between the MBQC and integrable phases. When $(\Delta + V_0)T \approx 2K\pi$ (K is an integer), many-body dynamics thermalize rapidly, as shown by the stroboscopic evolution of (b) mean energy $\langle \hat{H}_a \rangle$ and (c) population $\langle \hat{S}_z \rangle$. Here, $\langle \hat{H}_a \rangle \approx \epsilon_N/2$, and $\langle \hat{S}_z \rangle \approx 0$ in the thermalization phase (after about $n > 100$ Floquet period). In the integrable phase, the energy and population are largely unchanged from the initial state. Parameters are $N = 14$, $\Omega_0 = 1$, $V_0 = 2$, and $\tau = \pi$. See text for details.

conditions, as depicted in Fig. 1(a). Atoms in ground state $|g\rangle$ are excited to Rydberg state $|nS\rangle$ (with principal quantum number n and orbital angular momentum $l = 0$), which we denote as $|s\rangle$ for simplicity. The excitation is driven by a periodic Rabi frequency $\Omega(t)$. The Hamiltonian of the many-body system reads ($\hbar \equiv 1$)

$$\hat{H} = \frac{\Omega(t)}{2} \sum_j^N \hat{\sigma}_j^x + \Delta \sum_j^N \hat{n}_j + \sum_{j<k}^N V_{jk} \hat{n}_j \hat{n}_k, \qquad (1)$$

where Δ is the detuning, and operator $\hat{\sigma}_j^x = |g_j\rangle\langle s_j| + |s_j\rangle\langle g_j|$ and $\hat{n}_j = |s_j\rangle\langle s_j|$ are the Pauli matrix and projection operator of the Rydberg state, respectively. Atoms in the Rydberg state interact via the vdW interaction, $V_{jk} = \frac{V_0}{|j-k|^6}$, where $V_0 = C_6/a^6$ is the NN interaction ($C_6 \propto n^{11}$ and a to be the dispersion coefficient and lattice spacing). In what follows, we scale the Hamiltonian and time by Ω_0 and $1/\Omega_0$ except when discussing the experimental realization.

We employ a Floquet driving scheme where the Rabi frequency $\Omega(t)$ is shaped to be a square wave with strengths Ω_0 and Ω_l, and period $T = 2\tau$ [see Fig. 1(a)]. While we focus on $\Omega_l = 0$, our study is valid for any $|\Omega_0| \gg |\Omega_l|$, see Supplemental Material (SM) [83] for discussions (also including Refs. [14,17,84–98]). In Ref. [82], it has been shown that the square-wave modulation of laser detuning offers control over Rydberg atom interactions and entanglement dynamics. In our "bang-bang" protocol for the Rabi frequency, we achieve flexible control over the many-body phases and reveal thermalization-localization dynamics. Here, Hamiltonian (1) alternates between $\hat{H}_1 = \Omega_0/2 \sum_j \hat{\sigma}_j^x + \hat{H}_2$ and $\hat{H}_2 = \Delta \sum_j \hat{n}_j + \sum_{j<k} V_{jk} \hat{n}_j \hat{n}_k$. Dynamical evolution of the atoms is generated by the Floquet operator [17,99,100],

$$\hat{U}_F = e^{-i\hat{H}_2\tau} e^{-i\hat{H}_1\tau} = e^{-i\hat{H}_F T}, \qquad (2)$$

where $\hat{H}_F$ is the Floquet Hamiltonian [14]. In the high-frequency regime $\tau \ll 1$, we obtain an effective quantum spin model from the leading terms of the Magnus expansion (SM [83]). This model features Dzyaloshinsky-Moriya-type interactions, which could induce chiral and magnetic phases [101–103]. We will go beyond the high-frequency limit to regimes where finite-order expansions are generally insufficient to capture the physics.

Emergence of many-body quantum chaos. To understand the dynamics of the Floquet-driven Rydberg atom chain, we first diagonalize the Floquet operator to obtain its eigenphase θ_n and eigenstate $|\theta_n\rangle$, $\hat{U}_F|\theta_n\rangle = e^{-i\theta_n}|\theta_n\rangle$ ($n = 1, \cdots \mathcal{D}$), where $\mathcal{D}$ is the dimension of Hamiltonian $\hat{H}$ [104]. The eigenphases, $\theta_{\mathcal{D}} \geqslant \theta_{\mathcal{D}-1} \geqslant \cdots \geqslant \theta_1$, are unfolded in the interval $[0, 2\pi)$ and related to quasienergies ε_n through $\theta_n = \varepsilon_n T$. The level spacing ratio, $r_n = [\min(\delta_n, \delta_{n+1}]/[\max(\delta_n, \delta_{n+1})]$ between two consecutive eigenphases $\delta_n = \theta_{n+1} - \theta_n$, captures signatures of quantum chaos [29,105,106]. For $N \to \infty$, its average converges to $\langle r \rangle \approx 0.527$ (chaotic) when the distribution of θ_n is described by COE [107], and to $\langle r \rangle \approx 0.386$ (integrable) with Poisson (POI) distribution [23,108].

Due to the flexible control over laser and Rydberg interactions, we focus on an optimal situation where $V_0/\Omega_0 = K$, i.e., the NN interaction is K times the Rabi frequency Ω_0 (K to be an integer). This is important for controlling the integrable-chaos property of the Floquet-driven atom system [83]. As an example, the average ratio $\langle r \rangle$ is shown in Fig. 2(a) for parameters $\tau = \pi$ and $V_0 = 2$. Here, $\langle r \rangle$ distributes (almost) symmetrically with respect to a shifted detuning $\Delta_0 = \Delta + V_0 = 0$. There is a broad region, $-2 < \Delta_0 < 2$, where $\langle r \rangle$ is approximately 0.527, i.e., the eigenphase shows COE statistics. By increasing $|\Delta_0|$, we observe a series of narrow peaks $\langle r \rangle \approx 0.527$ when Δ_0 is near an integer, corresponding to the COE [Fig. 2 (b1)]. Between two neighboring peaks, $\langle r \rangle$ is low and close to that of the POI distribution, as illustrated in Fig. 2 (b2). For the open-ended chain, the profile of the level spacing statistics is almost identical for both the even and odd parity sectors [Fig. 2(a)] [83].

To understand the mechanism of quantum chaos at these peaks, we note that the undriven Hamiltonian (e.g., set $\Omega_0 = 0$ in $\hat{H}$) is fully given by the classical Hamiltonian $\hat{H}_2$. Its diagonal matrix elements are approximately integers owing to the optimal parameter. In other words, the unperturbed energies of many-body basis states $|j\rangle$ are approximately integers. For example, considering basis state $|\phi_N\rangle = |ss\cdots ss\rangle$ (all atoms in state $|s\rangle$), we obtain its expectation value, $\epsilon_N = \langle\phi_N|\hat{H}_2|\phi_N\rangle = N[\Delta + V_0 L_6(N-1) - V_0 L_5(N-1)/N]$ where $L_n(N) = \sum_{j=1}^N j^{-n}$ is the so-called Harmonic number of order n. For $N \gg 1$, $L_5(N-1)/N \to 0$, and $1 < L_6(N) < L_6(\infty) = \pi^6/945 \approx 1.017$. Here, the small decimal part in the latter results from the tails of the vdW interactions. Neglecting these contributions, we find that $\epsilon_N/N \approx \Delta_0$, which becomes an integer if Δ_0 is an integer. The diagonal elements of $\hat{H}_2$ are around integers independent of N. We emphasize that the vdW interaction tails only slightly

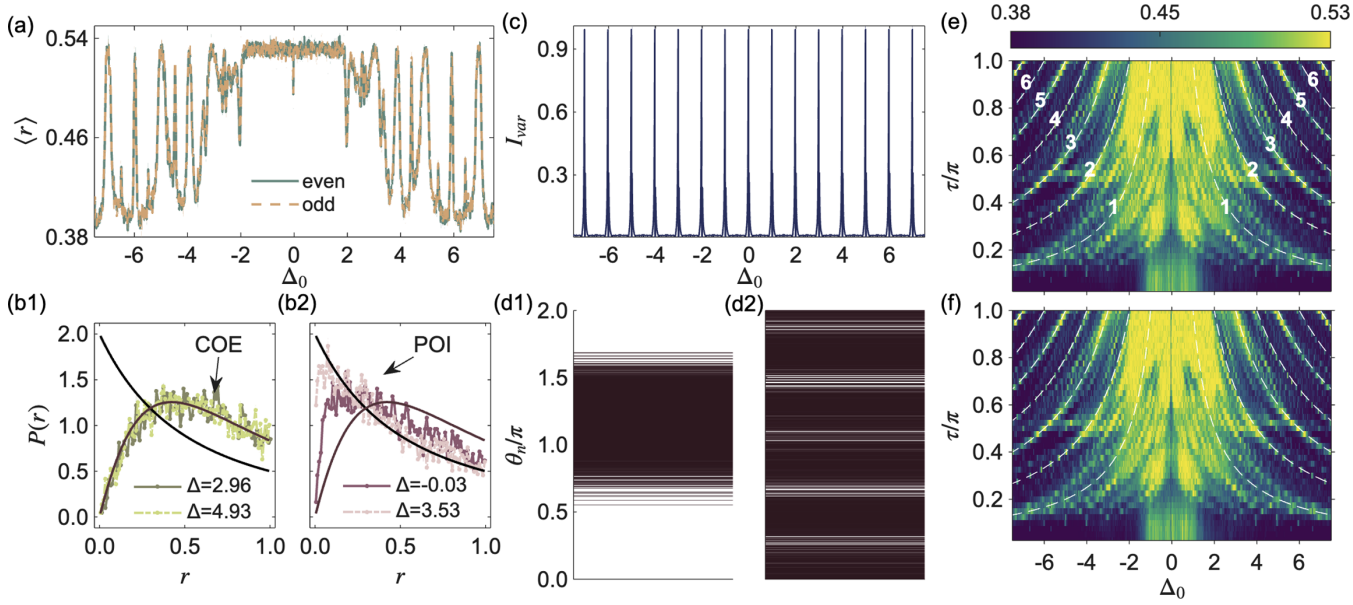


FIG. 2. (a) Profile of $\langle r\rangle$ as a function of Δ_0. When $|\Delta_0| > 2$, a series of chaos peaks, located around integer Δ_0, symmetrically distribute with respect to Δ_0. The even (solid) and odd (dotted) parity sectors have similar shapes and sizes. At the peaks, the level spacing exhibits COE statistics (b1), while it becomes largely a POI distribution (b2) at the lowest values (in the middle of two adjacent peaks). (c) Spreading of phase $\bar{\theta}_n$ of the undriven Hamiltonian $\hat{H}_2$. We show $I_{var} = I_0/\mathrm{Var}(\bar{\theta}_n)$ with $\mathrm{Var}(\bar{\theta}_n)$ to be the variance of $\bar{\theta}_n$ and $\bar{\theta}_n$ is the average value of quasiphase θ_n over all eigenstates. We normalize $\mathrm{Var}(\bar{\theta}_n)$ to be I_0 such that the maximal I_{var} is 1. It can be seen that I_{var} peaks when Δ_0 is an integer. (d) Distribution of eigenphase θ_n of the Floquet operator. The envelope of θ_n is a Gaussian (d1) at the chaos peak, while it is banded (d2) at the valley of $\langle r\rangle$. Diagrams of $\langle r\rangle$ as a function of Δ_0 and τ for even (e) and odd (f) sectors. The dashed curves, $\Delta_0 T = 2K\pi$, highlight the locations of the peaks. $|K|$ denotes the order of the reciprocal Floquet thermalization. In panels (a)–(d), $N = 14$ and $\tau = \pi$. In (e) and (f), $N = 12$. In all panels, $V_0 = 2$.

broaden the distributions of the unperturbed energies from the integers [Fig. 2(c)].

In the full Floquet operator, the laser ($\propto \hat{\sigma}_j^x$) couples the many-body basis states, generating a Gaussian envelope of θ_n [Fig. 2(d1)]. This is a key feature of chaotic systems [109]. As shown in Figs. 2(e) and 2(f), chaos peaks are found when $\Delta_0 T = 2K\pi$. This results in a series of *reciprocal quantum chaos* in the vicinity of $\Delta_0 T = 2K\pi$, in contrast to many previous studies where celebrated smooth integrable-to-chaos transitions are found [21,29,105,106,110]. Away from the chaos peak, the eigenvalues of $\hat{H}_2$ have broad distributions [Fig. 2(c)]. When the Floquet coupling is switched on, the distributions of eigenphase θ_n turn out to be banded [Fig. 2 (d2)]. Different bands form local subsystems, such that quantum chaos is prohibited [47].

We briefly make two remarks before proceeding to the next section. First, the qualitative difference between the regimes $|\Delta_0| < 2$ and $|\Delta_0| > 2$ originates from the way the drive couples to the banded quasienergy spectrum of $\hat{H}_2$. For small detuning, the drive strongly hybridizes multiple Floquet sidebands, effectively washing out the band structure and enabling rapid energy redistribution, which is indicative of quantum chaos. In contrast, when $|\Delta_0|$ exceeds this threshold, the band spacing becomes comparable to or larger than the Rabi coupling Ω_0, such that the drive predominantly couples near-resonant subbands. Second, a few lower peaks appear between two adjacent peaks corresponding to the reciprocal quantum chaos [for example, the one between $\Delta_0 \approx 4$ and 5 in Fig. 2(a)]. This is mainly attributed to the tail of the vdW interaction [83].

Reciprocal Floquet thermalization. We explore thermalization and localization by studying the stroboscopic dynamics of the Rydberg atom array. After n periods, expectation value $\langle\hat{O}\rangle(nT) = \langle\psi(nT)|\hat{O}|\psi(nT)\rangle$ of operator $\hat{O}$ is evaluated with stroboscopic state $|\psi(nT)\rangle = \hat{U}(nT)|\psi(0)\rangle$, where evolution operator $\hat{U}(nT) = [\hat{U}_F(T)]^n$. Normally, initial states typically lie in the middle region of the eigenspectrum [111,112] to ensure thermalization. These initial states are typically difficult to prepare experimentally. We employ two initial states $|\phi_0\rangle = |gg\cdots gg\rangle$, i.e., all atoms are state $|g\rangle$, and $|\phi_1\rangle = |+g\cdots+g\rangle$ with $|+\rangle = (|g\rangle + |s\rangle)/\sqrt{2}$, i.e., atoms are in superposition $|+\rangle$ and $|g\rangle$ alternatively in the array. These product states can be prepared experimentally [61,113].

We first show average population $\langle\hat{S}_z\rangle(nT) = \langle\psi(nT)|1/N\sum_j\hat{\sigma}_j^z|\psi(nT)\rangle$ in Fig. 1(c). In the chaotic regime, the population grows from -1 (-0.5) using the initial state $|\phi_0\rangle$ ($|\phi_1\rangle$). It reaches a steady value, around 0, as expected in a thermalizing state [114,115]. At the same time, the entanglement entropy saturates at the maximal possible value. We calculate the von Neumann entropy of subsystem A at stroboscopic time nT, $\mathcal{S}_{N_A}(nT) = -\mathrm{Tr}_A\,[\rho_A(nT)\ln\rho_A(nT)]$, where N_A ($N_B = N - N_A$) denotes the left (right) sites, and $\rho_A(nT) = \mathrm{Tr}_{N_B}(|\psi(nT)\rangle\langle\psi(nT)|)$ is the reduced density matrix of subsystem A. The half-chain entropy $\mathcal{S}_{N/2}$ saturates to the Page value $\langle\mathcal{S}_{N/2}\rangle = \ln 2^{N/2} - 1/2$ [116], as depicted in Fig. 3(a). Varying N_A, the saturated entropy increases linearly with $N_A < N/2$ [Fig. 3(b)] as a result of the volume law in thermal states [117].

In the integrable phase, the energy and population are confined to the initial values [Figs. 1(b) and 1(c)]. The

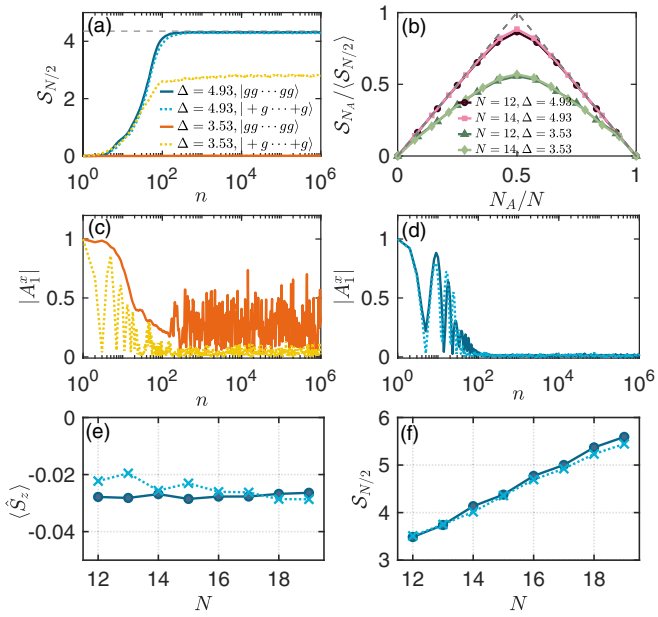


FIG. 3. (a) Stroboscopic dynamics of the half-chain entropy $\mathcal{S}_{N/2}$, which saturates to the Page value due to thermalization. (b) Saturated entanglement entropy of subsystem A. In the chaotic case $\Delta = 4.93$, the entropy follows the volume law and saturates to the Page value. In the integrable case $\Delta = 3.53$, the entropy is lower than the Page value. The entropies for $N = 12$ and 14 are almost identical in the corresponding phases. The entropy is averaged in the range $n \in [10^3, 10^4]$. Dynamics of $|A_1^x|$ in the integrable (c) and chaotic phase (d). The edge mode fluctuates strongly and persistently over time in (c). It decays quickly when the dynamics are thermalized. Saturated population $\langle\hat{S}_z\rangle$ (e) and half-chain entropy $\mathcal{S}_{N/2}$ (f) obtained using TDVP calculations for the chaotic case ($\Delta = 4.93$). In (a), (c), and (d), we consider $N = 14$. Other parameters are $V_0 = 2$ and $\tau = \pi$.

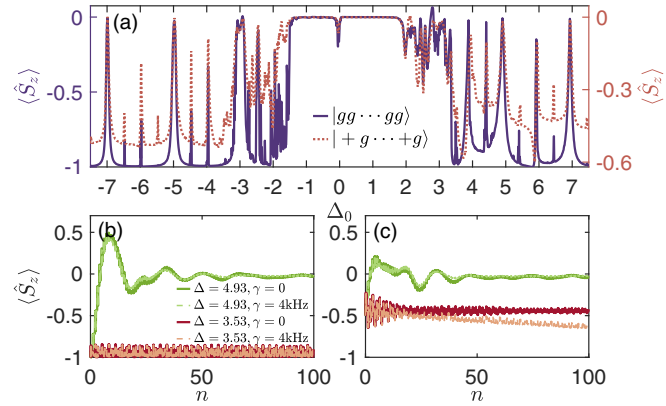


FIG. 4. (a) Average population $\langle\hat{S}_z\rangle$ for initial state $|\phi_0\rangle$ (left, solid line), and $|\phi_1\rangle$ (right, dotted line). Time evolution of the average population $\langle\hat{S}_z\rangle$ for initial states $|\phi_0\rangle$ (b) and $|\phi_1\rangle$ (c). Rydberg decay (dashed) plays a negligible role during the thermalization, but is state-dependent in the integrable regime. For state $|\phi_1\rangle$, the deviation results from the exponential decay of the Rydberg atoms in the otherwise frozen initial state. We consider $N = 14$ in panel (a) and $N = 12$ in panels (b) and (c). Other parameters are the same as in Fig. 3.

entanglement entropy is much lower than that of thermalization [Figs. 3(a) and 3(b)]. Despite the localization, strong fluctuations are found in edge modes, characterized by two-time correlation $|A_1^x| = \langle\psi(0)|\hat{\sigma}_1^x(nT)\hat{\sigma}_1^x|\psi(0)\rangle$ [118], as depicted in Fig. 3(c). In contrast, the edge mode decays to zero in the thermalizing phase [Fig. 3(d)].

Other quantities, such as autocorrelation [93], inverse participation ratio [89], and principal components [94], lead to consistent expectations with the population and entropy (see SM [83]). Moreover, we perform a finite-size scaling analysis in the thermal phase. In Figs. 3(e) and 3(f), we show saturated $\langle\hat{S}_z\rangle$ and $\mathcal{S}_{N/2}$ obtained using time-dependent variational principle (TDVP) calculations [91,92]. The former is approximately -0.02, while the latter increases with N in the thermal cases, indicating that the initial states cause robust thermalization dynamics [83].

Experimental probing of the thermalization and localization. As the population $\langle\hat{S}_z\rangle$ is sensitively dependent on the many-body phase, this provides a practical way to probe the reciprocal Floquet thermalization and localization dynamics. In Fig. 4(a), we show average population $\langle\hat{S}_z\rangle$ when the dynamics saturates. The sharp population peaks coincide with the thermalization peaks. In the integrable region, the average population is much smaller than 0. The distinctive population distribution thus encodes and provides a way to measure the level spacing statistics shown in Fig. 2(a).

Crucially, the dynamics of thermalization and localization remain observable within the finite lifetimes of Rydberg states. We demonstrate this using the $|60S\rangle$ state of Rb atoms, whose lifetime is 230 μs (decay rate $\gamma = 4.34$ kHz) and $C_6 \approx 139\ \text{GHz}\cdot(\mu\text{m})^6$ [95]. With a lattice spacing $a = 4.9\,\mu$m, the resulting NN interaction is $V_0 \approx 10$ MHz. For $\Omega_0 = 5$ MHz and $\tau = 0.2\pi\ \mu$s, this leads to $V_0/\Omega_0 = 2$, $\Omega_0 T = 2\pi$ and scaled decay rate $\gamma/\Omega_0 \approx 8 \times 10^{-4}$. We then solve the underlying master equation for the different phases [83]. As shown in Figs. 4(b) and 4(c), the decay has a negligible effect up to $n = 100$ (corresponding to 125.7 μs). Importantly, the saturation of the population is clearly visible. In Fig. 4(c), the deviation of the population in the integrable phase results from the exponential decay of the Rydberg component in the localized initial state. The consistent results provide a reliable basis for characterizing the two phases.

Conclusion and Discussion. We have investigated a Floquet scheme that enables the control of the reciprocal Floquet thermalization and localization dynamically in a one-dimensional Rydberg atom chain. The conditions to trigger and the mechanism of the thermalization are identified, which rely on the optimal combination of the strong vdW interaction and laser parameters. The vdW interaction is a key feature to generate the narrow chaos peaks, as other types of interactions (e.g., dipolar or Coulomb interactions) normally give broad chaos phases [83]. This reveals that the exponent of the interaction potential is a central parameter for controlling nonequilibrium dynamics and emergent phases [84]. We have also shown that thermalization and localization occur on experimentally accessible timescales and with the initial states used in Rydberg atom array experiments [83]. Future investigations using sophisticated approaches [119,120] may reveal the geometric origin of the reciprocal Floquet thermalization. The ability to control dynamical localization and thermalization has

potential applications in developing digital quantum simulation [55,56] with Rydberg atoms [70,121–126]. Our study furthermore opens opportunities to study edge modes [118], detect prethermalization [34,78], and engineer an effective many-body Hamiltonian using the Rydberg atom array setting [81,82].

Acknowledgments. We appreciate the insightful discussions with Marin Bukov, Keiji Saito, Tianyi Yan, Li You, Huanqian Loh, Yongqiang Li, and Thomas Pohl. This work was supported by the National Natural Science Foundation of China (Grants No. U2341211, No. 62175136, No. 12241408, and No. 12120101004); Innovation Program for Quantum Science and Technology (Grant No. 2023ZD0300902); Fundamental Research Program of Shanxi Province (Grant No. 202303021224007); and the 1331 project of Shanxi Province. W.L. acknowledges financial support from the EPSRC (Grant No. EP/W015641/1) and the Going Global Partnerships Programme of the British Council (Contract No. IND/CONT/G/22-23/26), and the use of the University of Nottingham's Ada HPC service.

Data availability. The data that support the findings of this article are openly available [127].

[1] D. A. Abanin, W. De Roeck, and F. Huveneers, Exponentially slow heating in periodically driven many-body systems, Phys. Rev. Lett. **115**, 256803 (2015).

[2] T. Mori, T. Kuwahara, and K. Saito, Rigorous bound on energy absorption and generic relaxation in periodically driven quantum systems, Phys. Rev. Lett. **116**, 120401 (2016).

[3] D. Abanin, W. De Roeck, W. W. Ho, and F. Huveneers, A rigorous theory of many-body prethermalization for periodically driven and closed quantum systems, Commun. Math. Phys. **354**, 809 (2017).

[4] A. Eckardt, Colloquium: Atomic quantum gases in periodically driven optical lattices, Rev. Mod. Phys. **89**, 011004 (2017).

[5] T. Oka and S. Kitamura, Floquet engineering of quantum materials, Annu. Rev. Condens. Matter Phys. **10**, 387 (2019).

[6] K. S. C. Decker, C. Karrasch, J. Eisert, and D. M. Kennes, Floquet engineering topological many-body localized systems, Phys. Rev. Lett. **124**, 190601 (2020).

[7] V. Borish, O. Marković, J. A. Hines, S. V. Rajagopal, and M. Schleier-Smith, Transverse-field Ising dynamics in a Rydberg-dressed atomic gas, Phys. Rev. Lett. **124**, 063601 (2020).

[8] S. Geier, N. Thaicharoen, C. Hainaut, T. Franz, A. Salzinger, A. Tebben, D. Grimshandl, G. Zürn, and M. Weidemüller, Floquet Hamiltonian engineering of an isolated many-body spin system, Science **374**, 1149 (2021).

[9] C. Weitenberg and J. Simonet, Tailoring quantum gases by Floquet engineering, Nat. Phys. **17**, 1342 (2021).

[10] B.-Y. Sun, N. Goldman, M. Aidelsburger, and M. Bukov, Engineering and probing non-Abelian chiral spin liquids using periodically driven ultracold atoms, PRX Quantum **4**, 020329 (2023).

[11] L. Zhang, Y. Ke, and C. Lee, Suppressing Floquet thermalization by driving transparency in tilted lattices, Phys. Rev. Res. **7**, 033206 (2025).

[12] R. Nandkishore and D. A. Huse, Many-body localization and thermalization in quantum statistical mechanics, Annu. Rev. Condens. Matter Phys. **6**, 15 (2015).

[13] M. Bukov, L. D'Alessio, and A. Polkovnikov, Universal high-frequency behavior of periodically driven systems: From dynamical stabilization to Floquet engineering, Adv. Phys. **64**, 139 (2015).

[14] T. Kuwahara, T. Mori, and K. Saito, Floquet–Magnus theory and generic transient dynamics in periodically driven many-body quantum systems, Ann. Phys. **367**, 96 (2016).

[15] J. Struck, M. Weinberg, C. Ölschläger, P. Windpassinger, J. Simonet, K. Sengstock, R. Höppner, P. Hauke, A. Eckardt, M. Lewenstein, and L. Mathey, Engineering Ising-XY spin-models in a triangular lattice using tunable artificial gauge fields, Nat. Phys. **9**, 738 (2013).

[16] M. Aidelsburger, M. Atala, M. Lohse, J. T. Barreiro, B. Paredes, and I. Bloch, Realization of the Hofstadter Hamiltonian with ultracold atoms in optical lattices, Phys. Rev. Lett. **111**, 185301 (2013).

[17] N. Goldman and J. Dalibard, Periodically driven quantum systems: Effective Hamiltonians and engineered gauge fields, Phys. Rev. X **4**, 031027 (2014).

[18] N. R. Cooper, J. Dalibard, and I. B. Spielman, Topological bands for ultracold atoms, Rev. Mod. Phys. **91**, 015005 (2019).

[19] J. Léonard, S. Kim, J. Kwan, P. Segura, F. Grusdt, C. Repellin, N. Goldman, and M. Greiner, Realization of a fractional quantum Hall state with ultracold atoms, Nature (London) **619**, 495 (2023).

[20] A. Russomanno, A. Silva, and G. E. Santoro, Periodic steady regime and interference in a periodically driven quantum system, Phys. Rev. Lett. **109**, 257201 (2012).

[21] L. Zhang, V. Khemani, and D. A. Huse, A Floquet model for the many-body localization transition, Phys. Rev. B **94**, 224202 (2016).

[22] P. Jurcevic, H. Shen, P. Hauke, C. Maier, T. Brydges, C. Hempel, B. P. Lanyon, M. Heyl, R. Blatt, and C. F. Roos, Direct observation of dynamical quantum phase transitions in an interacting many-body system, Phys. Rev. Lett. **119**, 080501 (2017).

[23] V. Khemani, A. Lazarides, R. Moessner, and S. L. Sondhi, Phase structure of driven quantum systems, Phys. Rev. Lett. **116**, 250401 (2016).

[24] D. V. Else, B. Bauer, and C. Nayak, Floquet time crystals, Phys. Rev. Lett. **117**, 090402 (2016).

[25] J. Zhang, P. W. Hess, A. Kyprianidis, P. Becker, A. Lee, J. Smith, G. Pagano, I.-D. Potirniche, A. C. Potter, A. Vishwanath, N. Y. Yao, and C. Monroe, Observation of a discrete time crystal, Nature (London) **543**, 217 (2017).

[26] A. Kyprianidis, F. Machado, W. Morong, P. Becker, K. S. Collins, D. V. Else, L. Feng, P. W. Hess, C. Nayak, G. Pagano, N. Y. Yao, and C. Monroe, Observation of a prethermal discrete time crystal, Science **372**, 1192 (2021).

[27] R. Moessner and S. L. Sondhi, Equilibration and order in quantum Floquet matter, Nat. Phys. **13**, 424 (2017).

[28] B. Ye, F. Machado and N. Y. Yao, Floquet phases of matter via classical prethermalization, Phys. Rev. Lett. **127**, 140603 (2021).
[29] L. D'Alessio and M. Rigol, Long-time behavior of isolated periodically driven interacting lattice systems, Phys. Rev. X **4**, 041048 (2014).
[30] A. Lazarides, A. Das, and R. Moessner, Equilibrium states of generic quantum systems subject to periodic driving, Phys. Rev. E **90**, 012110 (2014).
[31] S. A. Weidinger and M. Knap, Floquet prethermalization and regimes of heating in a periodically driven, interacting quantum system, Sci. Rep. **7**, 45382 (2017).
[32] H. Kim, T. N. Ikeda, and D. A. Huse, Testing whether all eigenstates obey the eigenstate thermalization hypothesis, Phys. Rev. E **90**, 052105 (2014).
[33] A. Haldar, R. Moessner, and A. Das, Onset of Floquet thermalization, Phys. Rev. B **97**, 245122 (2018).
[34] C. Fleckenstein and M. Bukov, Thermalization and prethermalization in periodically kicked quantum spin chains, Phys. Rev. B **103**, 144307 (2021).
[35] A. Morningstar, D. A. Huse, and V. Khemani, Universality classes of thermalization for mesoscopic Floquet systems, Phys. Rev. B **108**, 174303 (2023).
[36] C. B. Dağ, S. I. Mistakidis, A. Chan, and H. R. Sadeghpour, Many-body quantum chaos in stroboscopically-driven cold atoms, Commun. Phys. **6**, 136 (2023).
[37] R. Mukherjee, H. Guo, and D. Chowdhury, Floquet-thermalization via instantons near dynamical freezing, Phys. Rev. X **16**, 011041 (2026).
[38] J. Choi, H. Zhou, S. Choi, R. Landig, W. W. Ho, J. Isoya, F. Jelezko, S. Onoda, H. Sumiya, D. A. Abanin, and M. D. Lukin, Probing quantum thermalization of a disordered dipolar spin ensemble with discrete time-crystalline order, Phys. Rev. Lett. **122**, 043603 (2019).
[39] P. Peng, C. Yin, X. Huang, C. Ramanathan, and P. Cappellaro, Floquet prethermalization in dipolar spin chains, Nat. Phys. **17**, 444 (2021).
[40] L. S. Martin, H. Zhou, N. T. Leitao, N. Maskara, O. Makarova, H. Gao, Q.-Z. Zhu, M. Park, M. Tyler, H. Park, S. Choi, and M. D. Lukin, Controlling local thermalization dynamics in a Floquet-engineered dipolar ensemble, Phys. Rev. Lett. **130**, 210403 (2023).
[41] M. Lei, R. Fukumori, C.-J. Wu, E. Barnes, S. E. Economou, J. Choi, and A. Faraon, Quantum thermalization and Floquet engineering in a spin ensemble with a clock transition, Nat. Phys. **21**, 1196 (2025).
[42] R. V. Jensen and R. Shankar, Statistical behavior in deterministic quantum systems with few degrees of freedom, Phys. Rev. Lett. **54**, 1879 (1985).
[43] J. M. Deutsch, Quantum statistical mechanics in a closed system, Phys. Rev. A **43**, 2046 (1991).
[44] M. Srednicki, Chaos and quantum thermalization, Phys. Rev. E **50**, 888 (1994).
[45] M. Rigol, V. Dunjko, and M. Olshanii, Thermalization and its mechanism for generic isolated quantum systems, Nature (London) **452**, 854 (2008).
[46] P. Ponte, Z. Papić, F. Huveneers, and D. A. Abanin, Many-body localization in periodically driven systems, Phys. Rev. Lett. **114**, 140401 (2015).
[47] A. Lazarides, A. Das, and R. Moessner, Fate of many-body localization under periodic driving, Phys. Rev. Lett. **115**, 030402 (2015).
[48] D. A. Abanin, W. De Roeck, and F. Huveneers, Theory of many-body localization in periodically driven systems, Ann. Phys. **372**, 1 (2016).
[49] P. Bordia, H. Lüschen, U. Schneider, M. Knap, and I. Bloch, Periodically driving a many-body localized quantum system, Nat. Phys. **13**, 460 (2017).
[50] A. Morningstar, L. Colmenarez, V. Khemani, D. J. Luitz, and D. A. Huse, Avalanches and many-body resonances in many-body localized systems, Phys. Rev. B **105**, 174205 (2022).
[51] R. Yousefjani, S. Bose, and A. Bayat, Floquet-induced localization in long-range many-body systems, Phys. Rev. Res. **5**, 013094 (2023).
[52] P. Sierant, M. Lewenstein, A. Scardicchio, and J. Zakrzewski, Stability of many-body localization in Floquet systems, Phys. Rev. B **107**, 115132 (2023).
[53] R. Mukherjee, H. Guo, K. Lewellen, and D. Chowdhury, Arresting quantum chaos dynamically in transmon arrays, Newton **1**, 100011 (2025).
[54] K. Ji and B. V. Fine, Suppression of heating in quantum spin clusters under periodic driving as a dynamic localization effect, Phys. Rev. Lett. **121**, 050602 (2018).
[55] M. Heyl, P. Hauke, and P. Zoller, Quantum localization bounds Trotter errors in digital quantum simulation, Sci. Adv. **5**, eaau8342 (2019).
[56] L. M. Sieberer, T. Olsacher, A. Elben, M. Heyl, P. Hauke, F. Haake, and P. Zoller, Digital quantum simulation, Trotter errors, and quantum chaos of the kicked top, npj Quantum Inf. **5**, 78 (2019).
[57] D. A. Abanin, W. De Roeck, W. W. Ho, and F. Huveneers, Effective Hamiltonians, prethermalization, and slow energy absorption in periodically driven many-body systems, Phys. Rev. B **95**, 014112 (2017).
[58] L. Zhao, M. D. K. Lee, M. M. Aliyu, and H. Loh, Floquet-tailored Rydberg interactions, Nat. Commun. **14**, 7128 (2023).
[59] S. Basak, Y. Chougale, and R. Nath, Periodically driven array of single Rydberg atoms, Phys. Rev. Lett. **120**, 123204 (2018).
[60] S. K. Mallavarapu, A. Niranjan, W. Li, S. Wüster, and R. Nath, Population trapping in a pair of periodically driven Rydberg atoms, Phys. Rev. A **103**, 023335 (2021).
[61] L. Zhao, P. R. Datla, W. Tian, M. M. Aliyu, and H. Loh, Observation of quantum thermalization restricted to Hilbert space fragments and $\mathbb{Z}_{2k}$ scars, Phys. Rev. X **15**, 011035 (2025).
[62] T. L. Nguyen, J. M. Raimond, C. Sayrin, R. Cortiñas, T. Cantat-Moltrecht, F. Assemat, I. Dotsenko, S. Gleyzes, S. Haroche, G. Roux, Th. Jolicoeur, and M. Brune, Towards quantum simulation with circular Rydberg atoms, Phys. Rev. X **8**, 011032 (2018).
[63] C. J. Turner, A. A. Michailidis, D. A. Abanin, M. Serbyn, and Z. Papić, Weak ergodicity breaking from quantum many-body scars, Nat. Phys. **14**, 745 (2018).
[64] D. Bluvstein, A. Omran, H. Levine, A. Keesling, G. Semeghini, S. Ebadi, T. T. Wang, A. A. Michailidis, N. Maskara, W. W. Ho, *et al.*, Controlling quantum many-body dynamics in driven Rydberg atom arrays, Science **371**, 1355 (2021).
[65] S. Ebadi, T. T. Wang, H. Levine, A. Keesling, G. Semeghini, A. Omran, D. Bluvstein, R. Samajdar, H. Pichler, W. W. Ho,

S. Choi, S. Sachdev, M. Greiner, V. Vuletić, and M. D. Lukin, Quantum phases of matter on a 256-atom programmable quantum simulator, Nature (London) **595**, 227 (2021).

[66] P. Scholl, M. Schuler, H. J. Williams, A. A. Eberharter, D. Barredo, K.-N. Schymik, V. Lienhard, L.-P. Henry, T. C. Lang, T. Lahaye, A. M. Läuchli, and A. Browaeys, Quantum simulation of 2D antiferromagnets with hundreds of Rydberg atoms, Nature (London) **595**, 233 (2021).

[67] M. Saffman, Quantum computing with atomic qubits and Rydberg interactions: Progress and challenges, J. Phys. B: At. Mol. Opt. Phys. **49**, 202001 (2016).

[68] H. Levine, A. Keesling, G. Semeghini, A. Omran, T. T. Wang, S. Ebadi, H. Bernien, M. Greiner, V. Vuletić, H. Pichler, and M. D. Lukin, Parallel implementation of high-fidelity multiqubit gates with neutral atoms, Phys. Rev. Lett. **123**, 170503 (2019).

[69] D. Bluvstein, H. Levine, G. Semeghini, T. T. Wang, S. Ebadi, M. Kalinowski, A. Keesling, N. Maskara, H. Pichler, M. Greiner, V. Vuletić, and M. D. Lukin, A quantum processor based on coherent transport of entangled atom arrays, Nature (London) **604**, 451 (2022).

[70] T. M. Graham, Y. Song, J. Scott, C. Poole, L. Phuttitarn, K. Jooya, P. Eichler, X. Jiang, A. Marra, B. Grinkemeyer, M. Kwon, M. Ebert, J. Cherek, M. T. Lichtman, M. Gillette, J. Gilbert, D. Bowman, T. Ballance, C. Campbell, E. D. Dahl, *et al.*, Multi-qubit entanglement and algorithms on a neutral-atom quantum computer, Nature (London) **604**, 457 (2022).

[71] X.-Q. Shao, S.-L. Su, L. Li, R. Nath, J.-H. Wu, and W. Li, Rydberg superatoms: An artificial quantum system for quantum information processing and quantum optics, Appl. Phys. Rev. **11**, 031320 (2024).

[72] D. Bluvstein, S. J. Evered, A. A. Geim, S. H. Li, H. Zhou, T. Manovitz, S. Ebadi, M. Cain, M. Kalinowski, D. Hangleiter, J. P. Bonilla Ataides, N. Maskara, I. Cong, X. Gao, P. Sales Rodriguez, T. Karolyshyn, G. Semeghini, M. J. Gullans, M. Greiner, V. Vuletić, *et al.*, Logical quantum processor based on reconfigurable atom arrays, Nature (London) **626**, 58 (2024).

[73] J. Wu, J.-L. Wu, F.-Q. Guo, B.-B. Liu, S.-L. Su, X.-K. Song, L. Ye, and D. Wang, Quantum computation via Floquet tailored Rydberg interactions, npj Quantum Inf. **11**, 118 (2025).

[74] A. Browaeys and T. Lahaye, Many-body physics with individually controlled Rydberg atoms, Nat. Phys. **16**, 132 (2020).

[75] B. Mukherjee, A. Sen, D. Sen, and K. Sengupta, Dynamics of the vacuum state in a periodically driven Rydberg chain, Phys. Rev. B **102**, 075123 (2020).

[76] S. Sugiura, T. Kuwahara, and K. Saito, Many-body scar state intrinsic to periodically driven system, Phys. Rev. Res. **3**, L012010 (2021).

[77] B. Mukherjee, A. Sen, and K. Sengupta, Periodically driven Rydberg chains with staggered detuning, Phys. Rev. B **106**, 064305 (2022).

[78] S. Ghosh, D. Sen, and K. Sengupta, Detecting prethermal Floquet phases of Rydberg atom arrays, Phys. Rev. B **108**, 094302 (2023).

[79] N. Nishad, A. Keselman, T. Lahaye, A. Browaeys, and S. Tsesses, Quantum simulation of generic spin-exchange models in Floquet-engineered Rydberg-atom arrays, Phys. Rev. A **108**, 053318 (2023).

[80] W. S. Martins, F. Carollo, K. Brandner, and I. Lesanovsky, Quasiperiodic Floquet-Gibbs states in Rydberg atomic systems, Phys. Rev. A **111**, L010202 (2025).

[81] M. Tian, R. Samajdar, and B. Gadway, Engineering frustrated Rydberg spin models by graphical Floquet modulation, Phys. Rev. Lett. **135**, 253001 (2025).

[82] N. U. Koyluoglu, N. Maskara, J. Feldmeier, and M. D. Lukin, Floquet engineering of interactions and entanglement in periodically driven Rydberg chains, Phys. Rev. Lett. **135**, 113603 (2025).

[83] See Supplemental Material at http://link.aps.org/supplemental/10.1103/3gpm-9psv for details about level spacing ratio, effective Hamiltonian, and more illustrations, which also includes Refs. [14,17,84–98].

[84] M. Müllenbach, S. Geier, A. Braemer, E. Braun, T. Franz, G. Zürn, M. Weidemüller, and M. Gärttner, Quantum information scrambling in strongly disordered Rydberg spin systems, arXiv:2512.19856.

[85] K. Xu, Z.-H. Sun, W. Liu, Y.-R. Zhang, H. Li, H. Dong, W. Ren, P. Zhang, F. Nori, D. Zheng, H. Fan, and H. Wang, Probing dynamical phase transitions with a superconducting quantum simulator, Sci. Adv. **6**, eaba4935 (2020).

[86] J. W. Britton, B. C. Sawyer, A. C. Keith, C.-C. J. Wang, J. K. Freericks, H. Uys, M. J. Biercuk, and J. J. Bollinger, Engineered two-dimensional Ising interactions in a trapped-ion quantum simulator with hundreds of spins, Nature (London) **484**, 489 (2012).

[87] P. Richerme, Z.-X. Gong, A. Lee, C. Senko, J. Smith, M. Foss-Feig, S. Michalakis, A. V. Gorshkov, and C. Monroe, Non-local propagation of correlations in quantum systems with long-range interactions, Nature (London) **511**, 198 (2014).

[88] J. G. Bohnet, B. C. Sawyer, J. W. Britton, M. L. Wall, A. M. Rey, M. Foss-Feig, and J. J. Bollinger, Quantum spin dynamics and entanglement generation with hundreds of trapped ions, Science **352**, 1297 (2016).

[89] F. Dukesz, M. Zilbergerts, and L. F. Santos, Interplay between interaction and (un)correlated disorder in one-dimensional many-particle systems: Delocalization and global entanglement, New J. Phys. **11**, 043026 (2009).

[90] G. Misguich, V. Pasquier, and J.-M. Luck, Inverse participation ratios in the XXZ spin chain, Phys. Rev. B **94**, 155110 (2016).

[91] J. Haegeman, J. I. Cirac, T. J. Osborne, I. Pižorn, H. Verschelde, and F. Verstraete, Time-dependent variational principle for quantum lattices, Phys. Rev. Lett. **107**, 070601 (2011).

[92] M. Fishman, S. White, and E. Stoudenmire, The ITensor software library for tensor network calculations, SciPost Phys. Codebases 4 (2022).

[93] S. Aditya, D. Dhar, and D. Sen, Subspace-restricted thermalization in a correlated-hopping model with strong Hilbert space fragmentation characterized by irreducible strings, Phys. Rev. B **110**, 045418 (2024).

[94] L. F. Santos, F. Borgonovi, and F. M. Izrailev, Chaos and statistical relaxation in quantum systems of interacting particles, Phys. Rev. Lett. **108**, 094102 (2012).

[95] E. Robertson, N. Šibalić, R. Potvliege, and M. Jones, ARC 3.0: An expanded Python toolbox for atomic physics calculations, Comput. Phys. Commun. **261**, 107814 (2021).

[96] P. Jordan and E. Wigner, Über das Paulische Äquivalenzverbot, Z. Phys. **47**, 631 (1928).
[97] K. Joel, D. Kollmar, and L. F. Santos, An introduction to the spectrum, symmetries, and dynamics of spin-1/2 Heisenberg chains, Am. J. Phys. **81**, 450 (2013).
[98] O. Howell, P. Weinberg, D. Sels, A. Polkovnikov, and M. Bukov, Asymptotic prethermalization in periodically driven classical spin chains, Phys. Rev. Lett. **122**, 010602 (2019).
[99] S. Blanes, F. Casas, J. A. Oteo, and J. Ros, The Magnus expansion and some of its applications, Phys. Rep. **470**, 151 (2009).
[100] P. Ponte, A. Chandran, Z. Papić, and D. A. Abanin, Periodically driven ergodic and many-body localized quantum systems, Ann. Phys. **353**, 196 (2015).
[101] M. Brockmann, A. Klümper, and V. Ohanyan, Exact description of magnetoelectric effect in the spin-1/2 XXZ chain with Dzyaloshinskii-Moriya interaction, Phys. Rev. B **87**, 054407 (2013).
[102] C. Radhakrishnan, I. Ermakov, and T. Byrnes, Quantum coherence of planar spin models with Dzyaloshinsky-Moriya interaction, Phys. Rev. A **96**, 012341 (2017).
[103] X. Jin, D. C. Liu, Y. Shi, A. M. Chen, and Y. H. Su, Quantum phase transitions in the spin-1/2 XXZ model with staggered γ interaction, Phys. Rev. E **111**, 014110 (2025).
[104] A. Eckardt and E. Anisimovas, High-frequency approximation for periodically driven quantum systems from a Floquet-space perspective, New J. Phys. **17**, 093039 (2015).
[105] V. Oganesyan and D. A. Huse, Localization of interacting fermions at high temperature, Phys. Rev. B **75**, 155111 (2007).
[106] Y. Y. Atas, E. Bogomolny, O. Giraud, and G. Roux, Distribution of the ratio of consecutive level spacings in random matrix ensembles, Phys. Rev. Lett. **110**, 084101 (2013).
[107] M. L. Mehta, *Random Matrices*, 3rd ed., Pure and Applied Mathematics, Vol. 142 (Elsevier/Academic Press, Amsterdam, San Diego, CA, 2004).
[108] A. Pal and D. A. Huse, Many-body localization phase transition, Phys. Rev. B **82**, 174411 (2010).
[109] F. Haake, *Quantum Signatures of Chaos*, Springer Series in Synergetics, Vol. 54 (Springer Berlin Heidelberg, Berlin, Heidelberg, 2010).
[110] M. Sonner, M. Serbyn, Z. Papić, and D. A. Abanin, Thouless energy across the many-body localization transition in Floquet systems, Phys. Rev. B **104**, L081112 (2021).
[111] E. J. Torres-Herrera and L. F. Santos, Effects of the interplay between initial state and Hamiltonian on the thermalization of isolated quantum many-body systems, Phys. Rev. E **88**, 042121 (2013).
[112] K. He and M. Rigol, Initial-state dependence of the quench dynamics in integrable quantum systems. III. Chaotic states, Phys. Rev. A **87**, 043615 (2013).
[113] R. Shen, T. Chen, M. M. Aliyu, F. Qin, Y. Zhong, H. Loh, and C. H. Lee, Proposal for observing Yang-Lee criticality in Rydberg atomic arrays, Phys. Rev. Lett. **131**, 080403 (2023).
[114] M. Bukov, M. Heyl, D. A. Huse, and A. Polkovnikov, Heating and many-body resonances in a periodically driven two-band system, Phys. Rev. B **93**, 155132 (2016).
[115] J. Ren, Q. Li, W. Li, Z. Cai, and X. Wang, Noise-driven universal dynamics towards an infinite temperature state, Phys. Rev. Lett. **124**, 130602 (2020).
[116] D. N. Page, Average entropy of a subsystem, Phys. Rev. Lett. **71**, 1291 (1993).
[117] J. M. Deutsch, Eigenstate thermalization hypothesis, Rep. Prog. Phys. **81**, 082001 (2018).
[118] D. J. Yates, Fabian H. L. Essler, and A. Mitra, Almost strong $(0, \pi)$ edge modes in clean interacting one-dimensional Floquet systems, Phys. Rev. B **99**, 205419 (2019).
[119] N. Regnault, S. Liu, and B. A. Bernevig, Integer characteristic polynomial factorization and Hilbert space fragmentation, arXiv:2210.08019.
[120] P. M. Schindler and M. Bukov, Geometric Floquet theory, Phys. Rev. X **15**, 031037 (2025).
[121] M. Saffman, T. G. Walker, and K. Mølmer, Quantum information with Rydberg atoms, Rev. Mod. Phys. **82**, 2313 (2010).
[122] H. Weimer, M. Müller, H. P. Büchler, and I. Lesanovsky, Digital quantum simulation with Rydberg atoms, Quantum Inf. Processing **10**, 885 (2011).
[123] A. Bohrdt, A. Omran, E. Demler, S. Gazit, and F. Grusdt, Multiparticle interactions for ultracold atoms in optical tweezers: Cyclic ring-exchange terms, Phys. Rev. Lett. **124**, 073601 (2020).
[124] M. Morgado and S. Whitlock, Quantum simulation and computing with Rydberg-interacting qubits, AVS Quantum Sci. **3**, 023501 (2021).
[125] X. Wu, X. Liang, Y. Tian, F. Yang, C. Chen, Y.-C. Liu, M. K. Tey, and L. You, A concise review of Rydberg atom based quantum computation and quantum simulation, Chin. Phys. B **30**, 020305 (2021).
[126] F. Cesa and H. Pichler, Universal quantum computation in globally driven Rydberg atom arrays, Phys. Rev. Lett. **131**, 170601 (2023).
[127] Y. He, Y. Jiao, J. Zhao, and W. Li, Raw and processed simulation data for "reciprocal Floquet thermalization in one dimensional Rydberg atom array", Zenodo (2025), https://zenodo.org/records/18779098.